ACADEMIC PRESS

Available online at www.sciencedirect.com
SCIENCE DIRECT

Journal of Sound and Vibration 261 (2003) 483–501

JOURNAL OF SOUND AND VIBRATION

www.elsevier.com/locate/jsvi

Application of discrete-time variable structure control in the vibration reduction of a flexible structure

Der-An Wang[1], Yii-Mei Huang*

Department of Mechanical Engineering, National Central University, Chung-Li, 320 Taiwan, ROC

Received 28 August 2001; accepted 30 April 2002

Abstract

This paper studies the application of using the discrete-time variable structure control method to reduce the vibration of the flexible structure. The structure is subjected to arbitrary, unmeasurable disturbance forces. The concept of independent modal space control is adopted, and the system is studied by the discrete-time model. Here, discrete sensors and actuators are used. We choose the modal filters as the state estimator to obtain the modal co-ordinates and modal velocities for the modal space control. A discrete-time variable structure controller with a disturbance force observer is adopted due to its distinguished robustness property of insensitiveness to parameter uncertainties and external disturbances. The included disturbance force observer can observe the unknown disturbance modal forces, which are used in the discrete-time variable structure control law to cancel out the excitations. The upperbound limitations of the unknown disturbances in the variable structure control, therefore, are no longer needed. The switching surface, in the discrete-time variable structure control system, is designed in an optimal sense. That is, along the switching surface, the cost function of the states is minimized. The investigation of this research focuses on the optimal switching surface design and the control performances of the discrete-time variable structure controller. The performance of estimating the disturbance modal forces and the robustness property of the control law are also discussed.

1. Introduction

Flexible structures vibration control is an important issue in many engineering applications, especially for the precise operation performances in aerospace systems, satellites, flexible

*Corresponding author. Tel : +886-3-426-7345; fax: 886-3-425-4501.
E-mail address: t330005@cc.ncu.edu.tw (Y.-M. Huang).
[1] Current address: Department of Automatic Control Engineering, Chung Chou Institute of Technology, Yuan-Lin, 510 Taiwan, ROC.

PII: S0022-460X(02)00994-X

manipulators, etc. The flexible structures usually have low flexible rigidity and small material damping ratio. A little excitation may lead to destructive large amplitude vibration and long vibration decay time. These can result in fatigue, instability and poor operation of the structures. The earliest vibration control attempts began with passive methods. The passive vibration control methods employ the passive elements, e.g., masses, dampers and springs, to adjust the characteristics of controlled structures to the desired values. But the passive control methods can only control the structure responses up to a certain limit. When a better control performance is required, an active vibration control is needed. Different from the passive systems, the active vibration control supplies energy to suppress the vibration. However, the active vibration control system is more complicated than the passive system. The implementation of active vibration control needs lots of techniques about the measurement system, actuator elements and the controller design. Recently, with the advancements in the fast-calculating computer hardware, actuators/sensors techniques and the application of advanced control theories, real-time control of vibration becomes practical.

The active vibration control of flexible structures has been a research area of wide interest during the past several decades. Balas [1] and Meirovitch et al. [2,3] proposed the concept of the independent modal space control (IMSC) for the flexible structures, where the structures were discretized by the modal expansion method and every mode is uncoupled and individually controlled. Experiments were carried out to verify the feasibility of the modal control [4,5], where the modal filters [3,4,6] were used as the state estimator. Furthermore, Baz and Poh [7,8] presented a modified independent modal space control method to determine the optimal locations, control gains and excitation voltage of the piezoelectric actuators. The IMSC method was also used to study the vibration control of flexible mechanisms [9,10]. Additionally, there were many researches about the application of intelligent structures [11,12], where the sensors and actuators were embedded within the structures and were co-ordinated through a control system. Recently, due to the advancements in sensor and actuator techniques, the vibration control of using intelligent structures has received a great deal of attraction. Two popular control laws, used for the vibration suppression, are the pole-placement method and the linear quadratic (LQ) control theory [1–10]. These methods are useful to suppress the structures vibration without disturbance forces excitation. However, when the structures are excited by external disturbances, the active control systems should employ other robust control laws to eliminate the influences of the undesired excitations. In this paper, we consider the vibration control of a flexible structure subjected to unmeasurable disturbance forces. The variable structure control (VSC) method is adopted here due to its distinguished robustness property. The variable structure control law is simpler relative to other robust control methods, and this control system is almost insensitive to parametric uncertainties and external disturbances [13–16]. However, the implementation of the variable structure control technique requires the prior knowledge of the upperbounds of the disturbances. The upperbounds are not easy to obtain, and sometimes these values can yield undesired over-conservative feedback control gains. Recently, Eun et al. [17] proposed a discrete-time variable structure controller (DVSC) with a disturbance force observer which can estimate the unknown disturbances within certain estimation errors. Then, the conventionally assumed upperbound restriction on the unknown is relaxed to the restriction of the changing rate of the unknown [17], which is generally a more lenient requirement. The discrete-time variable structure control method is adopted in our research.

In this paper, an active control procedure for reducing the vibration of a flexible structure subjected to arbitrary, unmeasurable disturbance forces is investigated. The modal filters are used as the state estimator of the modal space. In order to suppress the vibration due to the external excitations, the discrete-time variable structure control law with a disturbance force observer is applied here. The disturbance force observer can estimate the unknown disturbance modal forces. These estimated values are used in the control law to cancel out the undesired excitations. The switching surface in the discrete-time variable structure control system is designed in an optimal sense. When the state trajectory is moving along the switching surface to the origin, the defined performance index of the states will be minimized. The discussions are concentrated on the optimal switching surface design, the effect of observing the disturbance modal forces and the control performances of the discrete-time variable structure control system.

2. Equation of motion

The flexible structure considered in this paper is a slender cantilever beam. As shown in Fig. 1, the beam has a constant cross-sectional area and the length of the beam is L. The axial direction is defined as the x-axis and t represents time. Displacement in the transverse direction is denoted as $y(x,t)$. The distributed excitation force acting on the beam is $P(x,t)$. The equation of motion of the beam can be expressed as [18]

$$EI\frac{\partial^4 y}{\partial x^4} + m\frac{\partial^2 y}{\partial t^2} = P(x,t), \tag{1}$$

where the Euler beam model is used. The notation E is Young's modulus of the beam material, I is the area moment of inertia of the beam cross-section m is the mass per unit length. Defining the following dimensionless parameters

$$y^* = y/L, \quad x^* = x/L, \quad t^* = (\sqrt{EI/m}/L^2)t, \quad P^* = (L^3/EI)P(x,t), \tag{2}$$

we have the non-dimensional equation of motion

$$\frac{\partial^4 y^*}{\partial x^{*4}} + \frac{\partial^2 y^*}{\partial t^{*2}} = P^*. \tag{3}$$

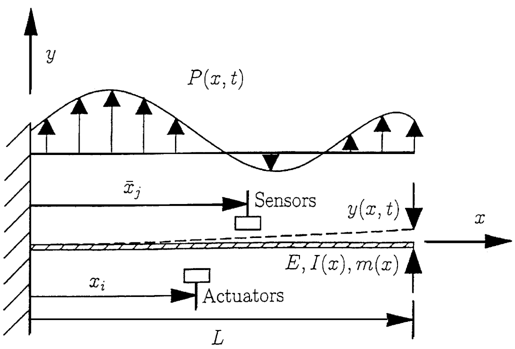

Fig. 1. Cantilever beam model with the dislocation sensors and actuators.

The normalized mode shape corresponding to the rth mode of the dimensionless cantilever beam is written as

$$\begin{aligned} Y_r^* = A_r^*(\sin\beta_r^* - \sinh\beta_r^*)(\sin\beta_r^* x^* - \sinh\beta_r^* x^*) \\ + (\cos\beta_r^* + \cosh\beta_r^*)(\cos\beta_r^* x^* - \cosh\beta_r^* x^*) \end{aligned} \tag{4}$$

with $r = 1, 2, 3, \ldots$ and A_r^* is a constant. In the last expression, the rth eigenvalue of the dimensionless beam β_r^* should satisfy the characteristic equation $\cos\beta_r^* \cosh\beta_r^* = -1$. The natural frequency of the rth mode is $\omega_r^* = \beta_r^* 2$. For obtaining the time responses of the dimensionless beam subjected to the dimensionless distributed force P^*, the method of truncated modal expansion is adopted here. The dimensionless displacement of the beam is approximately expressed as

$$y^* = \sum_{r=1}^{n} Y_r^* \eta_r^*, \tag{5}$$

where η_r^* is the rth modal co-ordinate, and n is the number of modes used. An extra uncoupled modal damping term of damping ratio ξ_r^* is added to each modal equation for representing the structure damping. A set of uncoupled modal equations then can be obtained as

$$\ddot{\eta}_r^* + 2\xi_r^* \omega_r^* \dot{\eta}_r^* + \omega_r^* 2\eta_r^* = n_r^*, \tag{6}$$

in which $r = 1, 2, \ldots, n$, and $n_r^* = \int_0^1 Y_r^* P^* \,\mathrm{d}x^*$ is the corresponding modal force. In the following section all the statements are discussed in this dimensionless system.

3. Independent modal space control

The scheme of control applied to the flexible beam here is based on the IMSC method [1–3]. In this method, every mode of the beam is independent to each other and is individually controlled. The discrete-time control system is considered. The schematic diagram of the beam vibration control is shown in Fig. 2(a). The beam displacements and velocities are measured by discrete sensors and are sampled through the analog-to-digital (A/D) converter. Then, the data are treated through the modal filters to obtain the modal co-ordinates and modal velocities. The feedback control algorithm is applied in the modal space. A discrete-time variable structure controller with a disturbance force observer [17] is developed. The observer provides the observed disturbance modal forces. The unwanted excitation can be eliminated by the proposed DVSC. The digital-to-analog (D/A) converter is added at the inputs of point actuators. Through the D/A converter, the modal control forces obtained from the DVSC are transferred to the point actuators to suppress the beam vibration.

3.1. Independent modal space control

Since the distributed force P^* applied to the beam is the sum of the unmeasurable disturbance forces and the control forces, the rth modal force n_r^* of the beam can also be separated into two portions. One is the control modal force n_{cr}^* and the other is the disturbance modal force n_{dr}^*. Here, n_{dr}^* is a bounded input, but the bound is unknown.

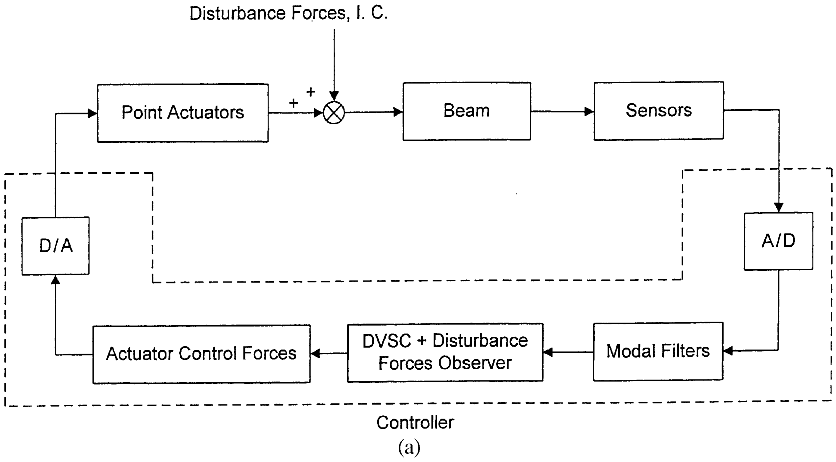

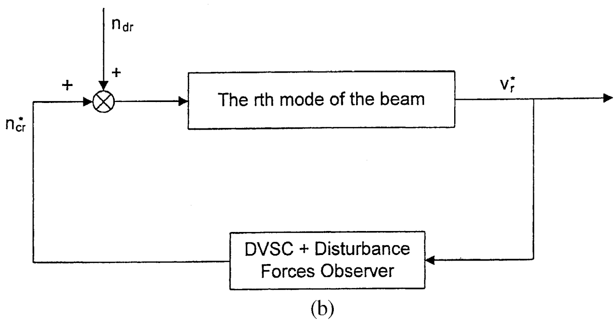

Fig. 2. Modal space vibration control block diagram of the beam: (a) schematic diagram of the beam vibration control; (b) the control block diagram of the rth mode of the beam.

Each modal equation (6) can be rearranged in the discrete-time state space form

$$\mathbf{v}_r(k+1) = \mathbf{A}_r\mathbf{v}_r(k) + \mathbf{B}_r n^*_{cr}(k) + \boldsymbol{\Gamma}_r n^*_{dr}(k), \tag{7}$$

in which $\mathbf{v}_r(k) = \begin{bmatrix} \eta^*_r(k) & \dot{\eta}^*_r(k) \end{bmatrix}^{\mathrm{T}}$, and $\mathbf{A}_r$, $\mathbf{B}_r$, $\boldsymbol{\Gamma}_r$ are the 2×2, 2×1, 2×1 matrices, respectively. According to the method of IMSC [2,3], each vibration mode is decoupled and is separately controlled. For reducing the influence of disturbance excitation $n^*_{dr}(k)$, the control modal force $n^*_{cr}(k)$ is derived from the discrete-time variable structure control law with a disturbance force observer. Fig. 2(b) shows the block diagram of the control of the rth mode.

3.2. Modal filters and point actuators forces

The implementation of the IMSC in the distributed structure requires the distributed sensors and actuators to extract the modal co-ordinates and supply the control modal forces respectively. Since the distributed sensors and actuators are not always available, discrete sensors and point actuators are usually used. The estimated modal co-ordinates $\hat{\eta}^*_r(k)$ and modal velocities $\dot{\hat{\eta}}^*_r(k)$

based on discrete measurements are [3,6,19]

$$\hat{\eta}^*_r(k) = \sum_{j=1}^{p} (\mathbf{D}^{*^{-1}})_{rj} y^*(\bar{x}^*_j, k),$$

$$\dot{\hat{\eta}}^*_r(k) = \sum_{j=1}^{p} (\mathbf{D}^{*^{-1}})_{rj} \dot{y}^*(\bar{x}^*_j, k), \tag{8}$$

where $r, j = 1, 2, \ldots, p$ and $\bar{x}^*_j$ is the jth sensor location. The matrix

$$\mathbf{D}^* = \begin{bmatrix} Y^*_1(\bar{x}^*_1) & Y^*_2(\bar{x}^*_1) & \cdots & Y^*_k(\bar{x}^*_1) \\ Y^*_1(\bar{x}^*_2) & Y^*_2(\bar{x}^*_2) & \cdots & Y^*_k(\bar{x}^*_2) \\ \vdots & \cdots & \cdots & \vdots \\ Y^*_1(\bar{x}^*_p) & Y^*_2(\bar{x}^*_p) & \cdots & Y^*_k(\bar{x}^*_p) \end{bmatrix}_{p \times p}. \tag{9}$$

Note that the inverse of $\mathbf{D}^*$ must exist. The estimated modal co-ordinates and modal velocities will replace $\eta^*_r(k)$ and $\dot{\eta}^*_r(k)$ used in the calculation of the control modal force $n^*_{cr}(k)$. The actual control forces are supplied by m discrete actuators located at x^*_i, $i = 1, 2, \cdots, m$, to control the first m modes of the beam. Then, the dimensionless control forces can be expressed as $\mathbf{F}^*(k) = \mathbf{Y}^{*^{-1}} \mathbf{N}^*_{\mathbf{c}}(k)$ [3,6,19], where

$$\mathbf{N}^*_{\mathbf{c}}(k) = \begin{bmatrix} n^*_{c1}(k) \\ n^*_{c2}(k) \\ \vdots \\ n^*_{cm}(k) \end{bmatrix}_{m \times 1}, \mathbf{Y}^* = \begin{bmatrix} Y^*_1(x^*_1) & Y^*_1(x^*_2) & \cdots & Y^*_1(x^*_m) \\ Y^*_2(x^*_1) & Y^*_2(x^*_2) & \cdots & Y^*_2(x^*_m) \\ \vdots & \vdots & \vdots & \vdots \\ Y^*_m(x^*_1) & Y^*_m(x^*_2) & \cdots & Y^*_m(x^*_m) \end{bmatrix}_{m \times m}, \mathbf{F}^*(k) = \begin{bmatrix} F^*_1(k) \\ F^*_2(k) \\ \vdots \\ F^*_m(k) \end{bmatrix}_{m \times 1} \tag{10}$$

and $F^*_i(k)$ is the ith dimensionless actuator force. The actuator locations x^*_i must be carefully chosen to avoid the singularity of $\mathbf{Y}^{*-1}$.

In structural vibration control, we will usually encounter the observation and control spillover. The observation spillover occurs when the unobserved modes responses are embedded into the modal filtering. This spillover effect can reduce the accuracy of estimated modal co-ordinates and modal velocities, and can also shift the uncontrolled modes eigenvalues when the feedback control is applied [1–3,6,20]. The observation spillover may even induce the instability of the system. The selection of sensor positions plays an important role in the phenomenon of observation spillover [3,6,20]. Usually, the lower vibration modes dominate the responses of structures. When the sensors are placed at the nodes of the lowest unobserved mode, the amplitude contribution of the unobserved modes to the modal filters can be greatly decreased. Consequently the observation spillover is reduced. Other useful ways to eliminate the observation spillover are using the prefilters to screen out the contribution of the unobserved modes or using more sensors to interpolate the modal co-ordinates precisely [1–3,6,20]. The other issue, control spillover, occurs when the uncontrolled modes are excited by the control forces for the controlled modes. The control spillover phenomenon can be reduced by placing the actuators at the nodes of the lowest uncontrolled mode [3]. The control spillover only degrades the performance of the control responses but cannot destabilize the system [1–3].

4. Discrete-time variable structure controller design

The controller adopted in this research is a discrete-time variable structure controller. Before designing the variable structure system, it is beneficial to introduce the characteristics of VSC and DVSC. Variable structure control with the sliding mode is an established method for controlling uncertain dynamics systems. The most attractive features of the VSC are invariance and robustness to uncertainties including model errors and external disturbances. This method enables the controller with a function of more than two structures, and the control is switched between different structures. The structures of the control law in the VSC system are governed by the sign of a specific switching function s where s is in terms of the states of the system [14–16,21,22]. The switching or sliding surface $s = 0$ divides the system phase plane into two regions, $s > 0$ and $s < 0$. All of the system state trajectories belong to one of the following situations: $s > 0$, $s = 0$ and $s < 0$. One of the conspicuous features of VSC is that any state trajectories outside the switching surface $s = 0$ will be forced to reach this surface, then slide on it and move to the system origin. The condition under which the state trajectory reaches the switching surface is called the reaching condition. The motion of the state trajectory under the reaching condition is called the reaching mode. The motion of the state trajectory slides on the switching surface is called the sliding mode which occurs by assuming that infinity fast switching between different structures is possible. Hence, the controller designed in VSC is to ensure that the reaching mode and sliding mode can occur and then the variable structure control is implemented.

The method of DVSC is similar to that of the continuous-time system. However, the discrete feature of the controller can cause zigzagging motion of the state trajectory near the switching surface instead of the motion sliding on the surface [14,16,23]. That is, DVSC can only undergo "quasi-sliding mode", and the states of the system can approach the switching surface but cannot stay on it, in general.

The first step of implementing VSC or DVSC algorithm is to design a stable switching surface which contains the desired closed-loop system dynamics. Then, design a variable structure control law such that the reaching and sliding modes can occur and the system is converging to its origin. In this section we will introduce the switching surface and the control law of the DVSC used in the research.

An optimal switching surface is considered here. In other words, if the state trajectory is moving along the switching surface, the defined quadratic performance index of states will be minimized. The discrete-time variable structure controller with a disturbance force observer [17] is adopted here. With the observer, the upperbounds assumption in the conventional DVSC can be relaxed. Thus, the controller is more non-conservative and sometimes the high gain input in the conventional DVSC can be alleviated [17,21,24]. The DVSC system is implemented in the modal space and every mode has a switching surface and the associated control modal force.

4.1. Optimal switching function design

There are many methods [14–16,21,22] to determine the switching function $s_r(k)$ of the rth modal equation. Note that the switching surface must contain the system origin. The major concern in designing the switching function is to guarantee that the system is stable and the states will approach to the origin when the state trajectory is in the quasi-sliding mode. One type of the switching surface $s_r(k) = 0$ is the optimal switching surface [21–23], which means that along the switching surface the defined quadratic performance index will be minimized when the state trajectory is in the sliding mode. Although the state trajectory is usually impossible to stay on the switching surface in DVSC, the optimal switching surface design can also give the sense to minimize the defined performance index [23].

Suppose the optimal switching function of the rth mode is defined as

$$s_r(k) = \mathbf{C}_r \mathbf{v}_r(k), \tag{11}$$

where $\mathbf{C}_r$ is a 1×2 matrix and will be determined later. For designing the optimal switching surface, a co-ordinate transformation is needed. The matrix $\mathbf{B}_r$ in Eq. (7) is a full rank matrix and this system is controllable. Let $\mathbf{z}_r(k) = [z_{1r}(k) \quad z_{2r}(k)]^{\mathrm{T}} = \mathbf{T}_r \mathbf{v}_r(k)$, where $\mathbf{T}_r$ is a 2×2 non-singular transformation matrix, so that $\mathbf{T}_r \mathbf{B}_r = [0 \quad \tilde{B}_{2r}]^{\mathrm{T}}_{1\times 2}$ with $\tilde{B}_{2r} \neq 0$. The properties of stability, controllability and observability of a linear system is invariable through this transformation. Thus, Eq. (7) can be rewritten as

$$\mathbf{z}_r(k+1) = \mathbf{T}_r \mathbf{A}_r \mathbf{T}_r^{-1} \mathbf{z}_r(k) + \mathbf{T}_r \mathbf{B}_r n^*_{cr}(k) + \mathbf{T}_r \boldsymbol{\Gamma}_r n^*_{dr}(k). \tag{12}$$

The transformed state space equation can be partitioned to yield

$$\begin{aligned} z_{1r}(k+1) &= \tilde{A}_{11r} z_{1r}(k) + \tilde{A}_{12r} z_{2r}(k) + \tilde{\Gamma}_{1r} n^*_{dr}(k), \\ z_{2r}(k+1) &= \tilde{A}_{12r} z_{1r}(k) + \tilde{A}_{22r} z_{2r}(k) + \tilde{B}_{2r} n^*_{cr}(k) + \tilde{\Gamma}_{2r} n^*_{dr}(k), \end{aligned} \tag{13}$$

where

$$\mathbf{T}_r \mathbf{A}_r \mathbf{T}_r^{-1} = \begin{bmatrix} \tilde{A}_{11r} & \tilde{A}_{12r} \\ \tilde{A}_{12r} & \tilde{A}_{22r} \end{bmatrix}_{2\times 2}, \quad \mathbf{T}_r \boldsymbol{\Gamma}_r = \begin{bmatrix} \tilde{\Gamma}_{1r} \\ \tilde{\Gamma}_{2r} \end{bmatrix}_{2\times 1}. \tag{14}$$

The switching function in the transformed system then becomes

$$s_r(k) = \mathbf{C}_r \mathbf{T}_r^{-1} \mathbf{z}_r(k). \tag{15}$$

In the design of the optimal switching function, it is usually assumed that the matching condition is held [21–23]. From the viewpoint of equivalent control [14,17,21,22], all of the perturbations are vanished in the sliding mode. Define the performance index of the controlled mode as [21–23]

$$\begin{aligned} J_r &= \sum_{k=k_s}^{\infty} \mathbf{z}_r^{\mathrm{T}}(k) \mathbf{Q}_r \mathbf{z}_r(k) \\ &= \sum_{k=k_s}^{\infty} (z_{1r}^{\mathrm{T}}(k) Q_{11r} z_{1r}(k) + 2 z_{1r}^{\mathrm{T}}(k) Q_{12r} z_{2r}(k) + z_{2r}^{\mathrm{T}}(k) Q_{22r} z_{2r}(k)), \end{aligned} \tag{16}$$

where

$$\mathbf{Q}_r = \begin{bmatrix} Q_{11r} & Q_{12r} \\ Q_{12r} & Q_{22r} \end{bmatrix}_{2\times 2}$$

is a positive definite matrix and k_s is the control step number when the sliding mode begins. Define the new variable $v_r(k)$ in the form of

$$v_r(k) = Q_{22r}^{-1} Q_{12r} z_{1r}(k) + z_{2r}(k). \tag{17}$$

The closed-loop dynamics of Eq. (13) in the sliding mode is then written as [21,22]

$$z_{1r}(k+1) = \tilde{A}^*_{11r} z_{1r}(k) + \tilde{A}_{12r} v_r(k) \tag{18}$$

and the performance index (16) becomes

$$J_r = \sum_{k=k_s}^{\infty} (z^{\mathrm{T}}_{1r}(k) Q^*_{11r} z_{1r}(k) + v^{\mathrm{T}}_r(k) Q_{22r} v_r(k)), \tag{19}$$

where

$$\tilde{A}^*_{11r} = \tilde{A}_{11r} - \tilde{A}_{12r} Q^{-1}_{22r} Q_{12r},$$

$$Q^*_{11r} = Q_{11r} - Q_{12r} Q^{-1}_{22r} Q_{12r}. \tag{20}$$

Eqs. (18) and (19) are the standard quadratic optimal control problem [21–23,25]. The solution in Ref. [25] can be applied directly. If $(\mathbf{A}_r\ \mathbf{B}_r)$ is controllable, then $(\tilde{A}^*_{11r}\ \tilde{A}_{12r})$ is also controllable [21,22]. The optimal control solution of Eqs. (18) and (19) is

$$v_r(k) = -K_r z_{1r}(k), \tag{21}$$

where

$$K_r = (Q_{22r} + \tilde{A}^{\mathrm{T}}_{12r} P_r \tilde{A}_{12r})^{-1} \tilde{A}^{\mathrm{T}}_{12r} P_r \tilde{A}^*_{11r} \tag{22}$$

and P_r is a p.d.s. solution of the standard discrete algebraic Riccati equation in the following form:

$$\tilde{A}^*_{11r}\mathrm{T} P_r \tilde{A}^*_{11r} - \tilde{A}^*_{11r}\mathrm{T} P_r \tilde{A}_{12r} (Q_{22r} + \tilde{A}^{\mathrm{T}}_{12r} P_r \tilde{A}_{12r})^{-1} \tilde{A}^{\mathrm{T}}_{12r} P_r \tilde{A}^*_{11r} - P_r = -Q^*_{11r}. \tag{23}$$

All of the eigenvalues of Eqs. (18) and (19) lie inside the unit circle. The system in the sliding mode is stable and is written as

$$z_{1r}(k+1) = (\tilde{A}^*_{11r} - \tilde{A}_{12r} K_r) z_{1r}(k). \tag{24}$$

Substituting Eq. (21) into Eq. (17), we have

$$(Q^{-1}_{22r} Q_{12r} + K_r) z_{1r}(k) + z_{2r}(k) = 0. \tag{25}$$

This is the sliding surface, $s_r(k) = \mathbf{C}_r \mathbf{T}^{-1}_r \mathbf{z}_r(k) = 0$, of the transformed system (12). We can determine the matrix $\mathbf{C}_r$ of the optimal switching function of the original system from Eq. (25).

4.2. Discrete-time variable structure control law with a disturbance force observer

The discrete-time variable structure control law with a disturbance force observer presented by Eun et al. [17] is adopted here. The major advantage of this method is that the conventionally assumed upperbound restriction on the disturbance force in DVSC is relaxed. The restriction now is on the changing rate of the disturbance. The optimal switching surface designed above could ensure that the closed-loop system in the quasi-sliding mode is stable and the states will converge to the origin if the control law satisfies the reaching condition. This in turn guarantees the existence of the quasi-sliding mode on the switching surface. The disturbance force estimation law and the discrete-time variable structure control law are as follows [17]:

$$\begin{aligned}\hat{n}^*_{dr}(k) &= \hat{n}^*_{dr}(k-1) + (\mathbf{C}_r\mathbf{B}_r)^{-1}g_r[s_r(k) - q_r s_r(k-1) + \kappa_r \mathrm{sgn}(s_r(k-1))],\\ n^*_{cr}(k) &= -\hat{n}^*_{dr}(k) + (\mathbf{C}_r\mathbf{B}_r)^{-1}[-\mathbf{C}_r\mathbf{A}_r\mathbf{v}_r(k) + q_r s_r(k) - \kappa_r \mathrm{sgn}(s_r(k))].\end{aligned} \tag{26}$$

The estimated disturbance modal force $\hat{n}^*_{dr}(k)$ is included in the control modal force $n^*_{cr}(k)$ to cancel out the disturbance excitation. The notations q_r, κ_r and g_r are constant parameters to be determined and $\mathrm{sgn}(\cdot)$ is the sign function. Similar to the reaching law method in Refs. [15,16,22], the parameter q_r is associated to the reaching rate of the reaching mode. The parameter κ_r is related to the disturbance force changing rate. By Eq. (26), the reaching mode and quasi-sliding mode of the controlled system can occur [17].

The closed-loop quasi-sliding mode dynamics of $s_r(k)$ is expressed as [17]

$$s_r(k+1) = q_r s_r(k) - \kappa_r\, \mathrm{sgn}(s_r(k)) + \mathbf{C}_r\mathbf{B}_r\Delta n^*_{dr}(k), \tag{27}$$

where $\Delta n^*_{dr}(k) = n^*_{dr}(k) - \hat{n}^*_{dr}(k)$ is the disturbance estimation error. The disturbance estimation error dynamics satisfies

$$\Delta n^*_{dr}(k+1) = (1-g_r)\Delta n^*_{dr}(k) + n^*_{dr}(k+1) - n^*_{dr}(k). \tag{28}$$

As proven in Refs. [17], if the disturbance changing rate $|n^*_{dr}(k+1) - n^*_{dr}(k)| < m_r$ holds for all k with $|1-g_r|<1$ and for some positive constant m_r, then there exists some k_0 such that $|\Delta n^*_{dr}(k)| \leqslant m_r/g_r$ for all $k > k_0$ regardless of $\Delta n^*_{dr}(0)$. It means that as the disturbance changing rate is bounded, the disturbance estimation error $\Delta n^*_{dr}(k)$ is less than a specific value. The magnitude of the switching function $s_r(k)$ is also proven to be bounded by the proposed control method [17]. It means that if the following conditions:

1. $0 \leqslant q_r \leqslant 1$, $0 < g_r < 1$
2. $|n^*_{dr}(k+1) - n^*_{dr}(k)| < m_r$ holds for all k for some constant $m_r > 0$
3. $\mathbf{C}_r\mathbf{B}_r(m_r/g_r) < \kappa_r$

are satisfied, the value of the switching function remains smaller than $\mathbf{C}_r\mathbf{B}_r(m_r/g_r) + \kappa_r$ regardless of the size of the disturbance force. When the disturbance varies slowly, m_r is small and accordingly small κ_r is sufficient to satisfy condition 3. This makes $\mathbf{C}_r\mathbf{B}_r(m_r/g_r) + \kappa_r$ being small and the value of the switching function is close to zero. The quasi-sliding mode then occurs in the neighborhood of the switching surface.

In variable structure control, chatter is inevitable because of the discontinuous control. To eliminate the chatter motion, a boundary layer around the switching surface is introduced [14,17,21,22]. A saturation function, $\mathrm{sat}(s_r(k)/\phi_r)$, can replace the sign function in Eq. (26) where ϕ_r is the thickness of the boundary layer [14,17,21,22]. Within the boundary layer, the control is a smooth approximation of the switching function. The stability of Eq. (12) is also guaranteed when the saturation function is used [17].

5. Numerical simulation and discussions

A cantilever beam subjected to unmeasurable disturbance forces is considered here. The investigation of the vibration control is carried out in the dimensionless system. The truncated beam model is adopted. The first 10 modes of the beam, including the controlled modes and uncontrolled modes, are used to represent the total beam responses in the numerical simulation. The damping ratio ξ_r^* of all modes are $\xi_r^* = 0.05$. According to IMSC for distributed structures, each mode is individually controlled. The modal filters are used as the state estimator. A discrete-time variable structure controller with a disturbance force observer is used to suppress the external excitation. The initial conditions of the beam are chosen as $y^*(1,0) = 1/3$, $\dot{y}^*(1,0) = 0$, and the disturbance force is applied at the tip of the beam. The ideal sensors and actuators used for the active vibration control dislocate to each other. The locations of actuators and sensors play a major role in the vibration control effect of structures. For using less actuator forces to control the structures vibration, good locations of the actuators are the points near the antinodes of the controlled mode shapes. The first four vibration modes are chosen as the controlled modes. The four actuators locations x_i^* are at $(0.29, 0.47, 0.69, 1.00)$, which are the points of the antinodes of the first three modes. For estimating the modal co-ordinates and velocities accurately, the first six modal co-ordinates and modal velocities are observed. The six sensors are distributed near the nodes of the seventh mode, then the observation spillover is greatly eliminated. The sensors locations $\bar{x}_j^*$ are at $(0.19, 0.35, 0.50, 0.65, 0.81, 0.95)$.

5.1. Estimated states by using modal filters

The purpose of using the modal filters is to obtain the modal co-ordinates and modal velocities. Fig. 3 shows the estimated modal co-ordinates from the modal filters for the first, fourth and the sixth modes, where the dimensionless disturbance force is $P^* = \sin t^*$ and no control is applied. The estimated modal co-ordinates are shown by the solid lines and the theoretical results are indicated by the dashed lines. From Fig. 3(a), it can be seen that the first estimated modal co-ordinate is almost the same as the theoretical value. Fig. 3(b) illustrates the fourth estimated modal co-ordinate where a small observation spillover is found. Fig. 3(c) shows the latest estimated modal co-ordinate, the sixth mode. Obviously, the observation spillover is large for this mode. In conclusion, the estimated modal co-ordinates of the lower modes are more accurate than the higher ones [6,19] and the observation spillover is more evident in higher modes.

5.2. Modal space vibration control by the discrete-time variable structure control method

The estimated modal co-ordinates and velocities by modal filters are used to calculate the values of the switching functions and to determine the control modal forces in the modal space vibration control. The point actuator forces are obtained according to the description in Section 3 after the modal co-ordinates and velocities are known. The first procedure of designing the discrete-time variable structure control law is to determine the stable switching function. Then, design the control law such that the reaching mode and quasi-sliding mode occur. The design of the DVSC for the beam system is presented below.

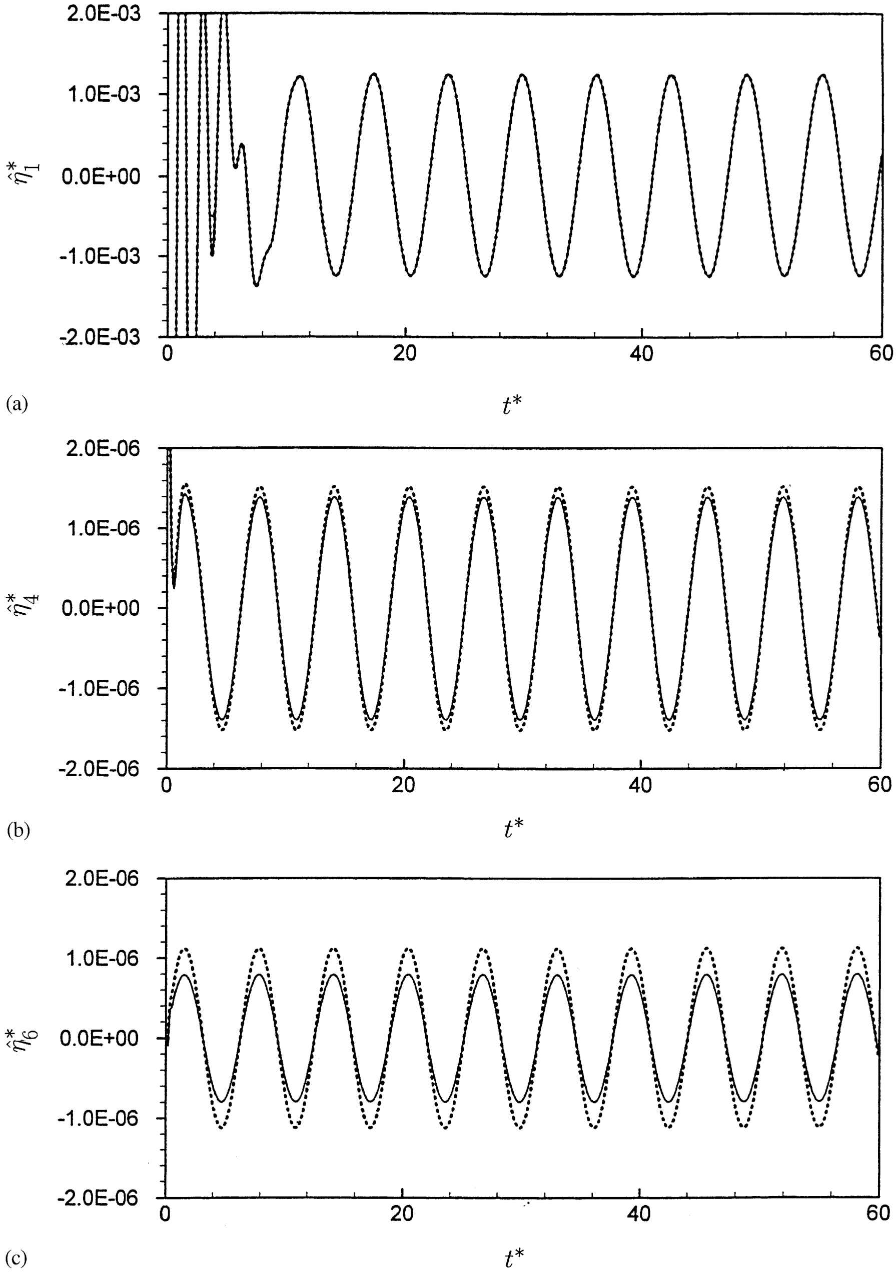

Fig. 3. Estimated modal co-ordinates by using modal filters: (a) the first mode; (b) the fourth mode; and (c) the sixth mode.

5.2.1. The optimal switching functions design

The modal Eq. (7) is controllable and the associated $\mathbf{B}_r$ is a full rank matrix. Every controlled mode has a switching function. The design objective of the optimal switching function is to find the switching surface such that the defined quadratic performance index of the controlled mode will be minimized when the state trajectory is in the sliding mode. For designing the optimal switching function, the modal Eq. (7) must be transformed to a new co-ordinates system. By choosing a simple non-singular transformation matrix

$$\mathbf{T}_r = \begin{bmatrix} 1 & -\frac{\mathbf{B}_{r,11}}{\mathbf{B}_{r,21}} \\ 0 & 1 \end{bmatrix},$$

where $\mathbf{B}_{r,11}$ and $\mathbf{B}_{r,21}$ are the elements of $\mathbf{B}_r$, the modal equation is transformed to the new co-ordinates system, Eq. (12). Suppose the quadratic performance index defined in the original system is $J_{or} = \sum_{k=k_s}^{\infty} \mathbf{v}_r^{\mathrm{T}}(k)\mathbf{Q}_{or}\mathbf{v}_r(k)$, where the subscript o refers to the original system. For balancing the weighting between modal co-ordinate and modal velocity in J_{or}, we choose

$$\mathbf{Q}_{or} = \begin{bmatrix} \omega_r^2 & 0 \\ 0 & 1 \end{bmatrix}.$$

Then the weighting matrix, in the new co-ordinates system, is $\mathbf{Q}_r = (\mathbf{T}_r^{-1})^{\mathrm{T}}\mathbf{Q}_{or}\mathbf{T}_r^{-1}$. By the definition of state variables given in Eq. (17), the minimization of the performance index J_r (16) becomes the standard discrete-time optimal control problem. Solving Eqs. (18) and (19), we obtain the associated optimal state feedback gain K_r. All the eigenvalues of $A_{11r}^* - A_{12r}K_r$ lie inside the unit circle. The switching surface of the new coordinates system is given in Eq. (25). By the inverse transformation, the coefficient matrix $\mathbf{C}_r$ of the optimal switching function of the original system is determined. Table 1 gives the associated optimal switching functions of the controlled modes.

5.2.2. Discrete-time variable structure control

The discrete-time variable structure control law with a disturbance force observer is used in the research. With the disturbance force observer observing the disturbance modal forces, the external excitation will be cancelled out by the estimated values. The upperbounds of the perturbations in the conventional DVSC are not needed. The condition now is relaxed to the restriction of the changing rates of the unknown disturbances. This is generally a more lenient requirement than the conventional requirement of bounded disturbances magnitudes. However, the chattering phenomenon is always encountered in the variable structure control. For eliminating the chattering, the boundary layer method is employed. The saturation functions $\mathrm{sat}(s_r(k)/\phi_r)$, with the boundary layers thickness ϕ_r, replace the sign functions in Eq. (26). Within the boundary layers, the control modal forces $n_{cr}^*(k)$ are more smooth than those without using the boundary layer method, and the chattering phenomena can be eliminated. Moreover, the values of $|s_r(k)/\phi_r|$

Table 1
Optimal switching functions of controlled modes

Mode no.	$s_r(k) = \mathbf{C}_r\mathbf{v}_r(k)$
1	$\mathbf{C}_1 = [3.5218 \quad 1]$
2	$\mathbf{C}_2 = [22.0657 \quad 1]$
3	$\mathbf{C}_3 = [61.4716 \quad 1]$
4	$\mathbf{C}_4 = [119.1794 \quad 1]$

Table 2
Design parameters of the discrete-time variable structure control law with a disturbance force observer

Mode no.	q_r	k_r	g_r	ϕ_r
1	0.73	4.7×10^{-3}	0.6	5×10^{-2}
2	0.65	5.1×10^{-4}	0.6	5×10^{-3}
3	0.52	6.3×10^{-5}	0.6	5×10^{-4}
4	0.47	7.5×10^{-6}	0.6	5×10^{-5}

are usually less than 1 within the boundary layers. It means that the control gains within the boundary layer are evidently reduced. The dimensionless sampling time of the DVSC system is chosen as 0.001. Suppose the disturbance modal forces changing rates m_r of the first four modes are less than $2^{-2}, 2^{-3}, 2^{-4}, 2^{-5}$, respectively. Table 2 gives the design parameters of the controller of different controlled modes. Since the higher modes dynamic responses are faster than those of the lower modes, q_r of higher modes are less than those of the lower modes for balancing the reaching time of each mode. The dynamic response amplitudes of higher modes are smaller than those of lower modes, so the associated values of κ_r and ϕ_r are also smaller. With the above design parameters, the disturbance estimation errors are bounded within certain acceptable values. The finite reaching time and the quasi-sliding mode properties are also guaranteed.

Fig. 4 demonstrates the performance of the disturbance force observer for observing different types of disturbance forces for the first mode. The effect of tracking the sine function, $\sin t^*$, is shown in Fig. 4(a). The solid line displays the observed disturbance modal force $\hat{n}^*_{d1}(k)$. The dashed line indicates the actual disturbance modal force $n^*_{d1}(k)$. Fig. 4(b) represents the result of observing the force $0.4 \sin t^* + 0.3\cos 2t^* + 0.3\sin(4t^* + 1)$, and Fig. 4(c) shows the result of observing the step function of amplitude 1. It is seen that the disturbance force observer can estimate the disturbance modal forces very well. Because of the short sampling time and the small changing rates m_1, the observed disturbance modal forces are almost the same as the real disturbance modal force. The more accurately the disturbance modal forces are observed, the better cancellation of these disturbance forces will be obtained when the control is implemented. When the estimation errors are small, the variations in the switching functions and the system oscillation are also small.

The control results of the first mode are illustrated in Fig. 5, where the disturbance force is $\sin t^*$. The solid lines indicate the controlled mode responses and the dashed lines exhibits the uncontrolled mode responses. From Fig. 5, the discrete-time variable structure control law with a disturbance force observer presented in this paper can successfully suppress the modal responses. The mode response is insensitive to the external excitation. There are almost no steady state oscillation found and without the often seen chattering phenomenon in DVSC due to the good accuracy of estimated disturbance modal force and the use of suitable saturation function.

With the optimal switching surface designed in Section 5.2.1 Fig. 6 exhibits the phase portraits of the controlled modes when the control is implemented. The reaching mode and quasi-sliding mode motions are clear in this figure. Because of the suitable choosing of the boundary layers thickness ϕ_r, the chattering phenomenon does not occur. The state trajectories are bounded within the boundary layers when they are in quasi-sliding mode. Note, the small estimation errors of

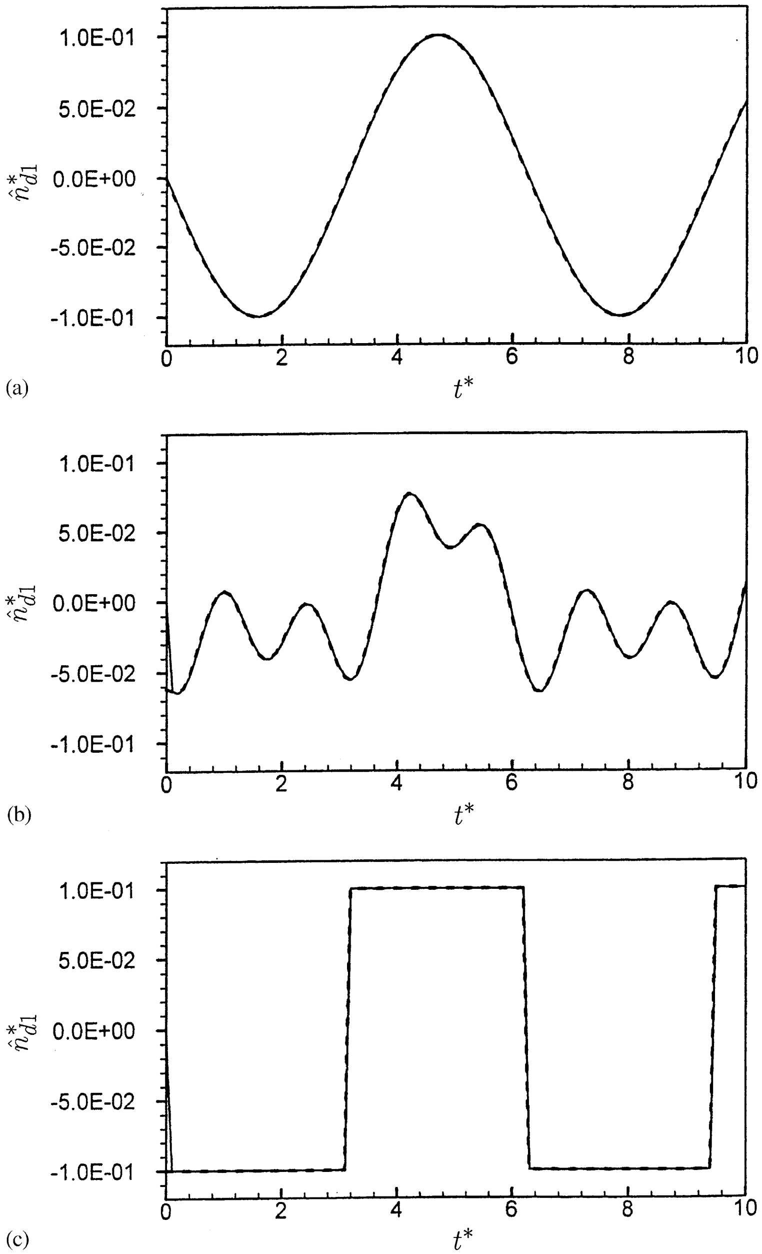

Fig. 4. Observed disturbance modal forces via the disturbance force observer: (a) sin t^*; (b) 0.4sin t^* + 0.3cos $2t^*$ + 0.3sin $(4t^* + 1)$; (c) step function of amplitude 1.

disturbance modal forces also induce small variations of $s_r(k)$ around the switching surfaces $s_r(k) = 0$. Although employing the saturation function can avoid the chattering, it also degrades the robustness of the control law and the control performance [14,21,22]. The states trajectories will oscillate around the origin of the system when we use the saturation functions. The oscillation

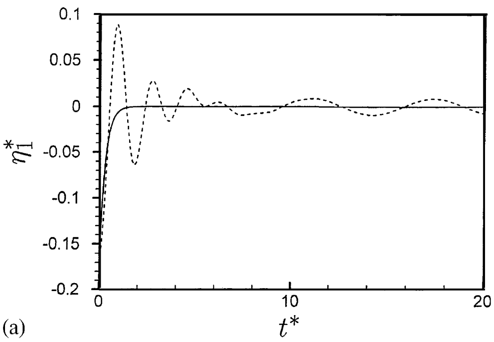

(a)

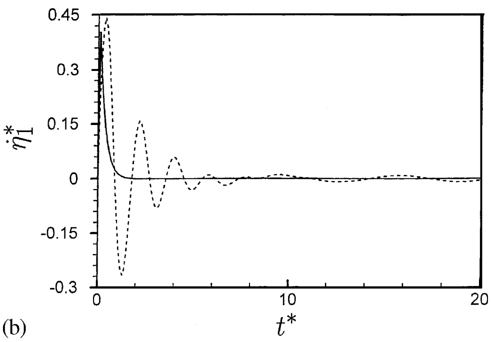

(b)

Fig. 5. Responses of the first mode under the discrete-time variable structure control with a disturbance force observer: (a) modal co-ordinate; (b) modal velocity.

phenomenon is not seen here due to the scale chosen in the figure. As the boundary layer thickness is increased, this phenomenon is expected to be more evident.

Fig. 7 illustrates both of the first control modal force and the first disturbance modal force. The circle symbol indicates the first control modal force and the dashed line indicates the first disturbance modal force. The chattering phenomenon is also not found in the control modal force. From this figure, we see that the control modal force cancel out the disturbance modal force effectively. Fig. 8 displays the control results of the beam. The solid lines indicate the controlled beam tip responses and the dashed lines exhibit the non-controlled beam tip responses. The vibration of the beam is quickly suppressed and the steady state oscillation is not found when the beam is controlled. The control spillover phenomenon of distributed system is not evident here due to the figure chosen. The discrete-time variable structure control law with a disturbance force observer can suppress the vibration well and the disturbance rejection ability is good.

6. Conclusions

The application of using the discrete-time variable structure control method to suppress the vibration of a flexible structure, subjected to unmeasurable disturbance forces, has been investigated. The independent modal space control is used as the frame of the vibration control of

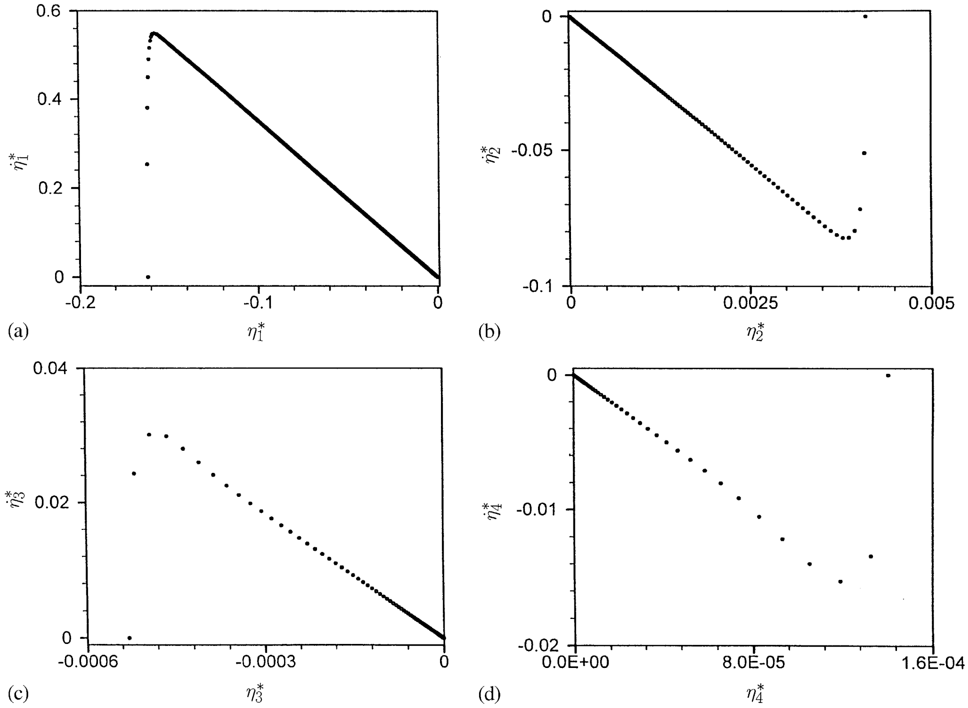

Fig. 6. Phase portraits of the controlled modes when the control is implemented. (a) the first mode; (b) the second mode; (c) the third mode; and (d) the fourth mode.

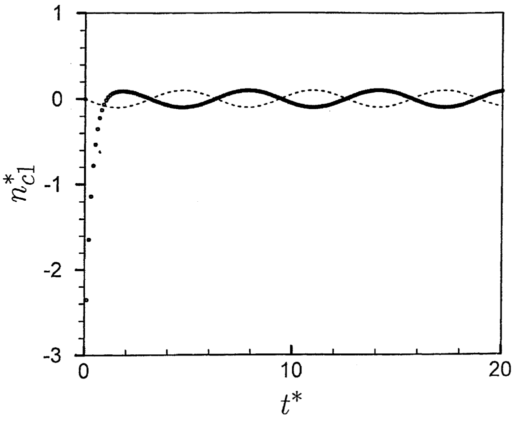

Fig. 7. First control modal force of the beam when the control is implemented.

the distributed parameters structure. The modal filters are used to estimate the modal co-ordinates. A discrete-time variable structure controller with a disturbance force observer, for each mode, is adopted due to its distinguished robustness property to against external excitations. This variable structure control technique can observe the unknown disturbances well. Then, the

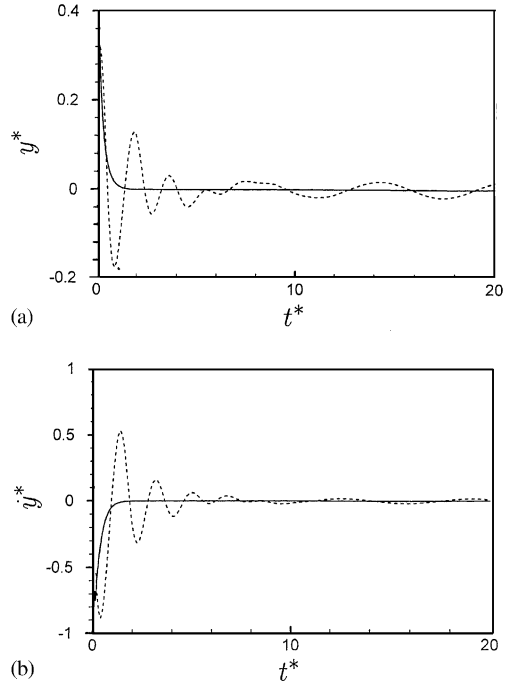

Fig. 8. Tip responses of the beam under the discrete-time variable structure control with a disturbance force observer: (a) tip displacement; and (b) tip velocity.

variations in the switching functions of controlled modes and the system oscillation are reduced. Moreover, the upperbounds criterion of the disturbances in the conventional DVSC is relaxed to the changing rates of the disturbances. The optimal switching surfaces are designed in the DVSC for minimizing the linear quadratic cost functions of states. The simulation results show that this control algorithm has good disturbance rejection ability and can successfully attenuate the structure vibration.

Acknowledgements

This work was sponsored by the National Science Council, ROC, under the Grant NCS 89-2212-E-008-038; this support is gratefully acknowledged.

References

[1] M.J. Balas, Modal control of certain flexible dynamic systems, SIAM Journal on Control and Optimization 16 (3) (1978) 450–462.
[2] L. Meirovitch, H. Baruh, Control of self-adjoint distributed-parameter systems, Journal of Guidance and Control 5 (1) (1982) 60–66.
[3] L. Meirovitch, Dynamics and Control of Structures, Wiley, New York, 1990.

[4] L. Meirovitch, H. Baruh, R.C. Montgomery, J.P. Williams, Nonlinear natural control of an experimental beam, Journal of Guidance, Control, and Dynamics 7 (4) (1984) 437–442.
[5] B.E. Schafer, H. Holzach, Experimental research on flexible beam modal control, Journal of Guidance, Control, and Dynamics 8 (5) (1985) 597–604.
[6] L. Meirovitch, H. Baruh, The implementation of modal filters for control of structures, Journal of Guidance, Control, and Dynamics 8 (6) (1985) 707–716.
[7] A. Baz, S. Poh, Performance of an active control system with piezoelectric actuators, Journal of Sound and Vibration 126 (2) (1988) 327–343.
[8] A. Baz, S. Poh, Experimental implementation of the modified independent modal space control method, Journal of Sound and Vibration 139 (1) (1990) 133–149.
[9] Zhang Xianmin, Liu Hongzhao, Caoweiqing, Active vibration control of flexible mechanisms, Chinese Journal of Mechanical Engineering 32 (1) (1996) 9–16.
[10] Shao Changjian, Zhang Xianmin, Complex mode active vibration control of high-speed flexible linkage mechanisms, Journal of Sound and Vibration 234 (3) (2000) 491–506.
[11] C.K. Lee, F.C. Moon, Modal sensors/actuators, ASME Journal of Applied Mechanics 57 (2) (1990) 434–441.
[12] D.J. Inman, Active modal control for smart structures, Philosophical Transactions of the Royal Society, Series A 359 (1778) (2001) 205–219.
[13] R.F. Fung, C.C. Liao, Application of variable structure control in the nonlinear string system, International Journal of Mechanical Sciences 37 (9) (1995) 985–993.
[14] J.Y. Hung, W. Gao, J.C. Hung, Variable structure control: a survey, IEEE Transactions on Industrial Electronics 40 (1) (1993) 2–22.
[15] W. Gao, J.C. Hung, Variable structure control of nonlinear systems: a new approach, IEEE Transactions on Industrial Electronics 40 (1) (1993) 45–55.
[16] W. Gao, Y. Wang, A. Homaifa, Discrete-time variable structure control systems, IEEE Transactions on Industrial Electronics 42 (2) (1995) 117–122.
[17] Y. Eun, J.H. Kim, D. Cho, Discrete-time variable structure controller with a decoupled disturbance compensator and its application to a CNC servomechanism, IEEE Transactions on Control Systems Technology 7 (4) (1999) 414–423.
[18] L. Meirovitch, Analytical Methods in Vibration, MacMillan, New York, 1967.
[19] D.A. Wang, Y.M. Huang, Modal space vibration control of a beam by using the feedforward and feedback control loops, International Journal of Mechanical Sciences 44 (1) (2002) 1–19.
[20] E.A. Czajkowski, A. Preumont, R.T. Haftks, Spillover stabilization of large space structures, Journal of Guidance, Control, and Dynamics 13 (6) (1990) 1000–1007.
[21] V.I. Utkin, Sliding Modes in Control and Optimization, Springer, Berlin, 1992.
[22] W.B. Gao, Foundation of Variable Structure Control, China Press of Science and Technology, Beijing, 1990 (in Chinese).
[23] A.J. Koshkouei, A.S.I. Zinober, Sliding mode control of discrete-time systems, transactions of the American society of mechanical engineering, Journal of Dynamic Systems, Measurement and Control 122 (4) (2000) 793–802.
[24] H. Elmali, N. Olgac, Implementation of sliding mode control with perturbation estimation (SMCPE), IEEE Transactions on Control Systems Technology 4 (1) (1996) 79–85.
[25] K. Ogata, Discrete-Time Control Systems, 2nd edn, Prentice-Hall, Englewood cliffs, NJ, 1995.